Forensic Imaging 36 (2024) 200579

Contents lists available at ScienceDirect

Forensic Imaging

journal homepage: www.sciencedirect.com/journal/forensic-imaging

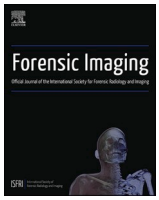

Technical note: Analysis of the auricular surface for age estimation using dirichlet normal energy

Jisun Jang [a,*], Enrico Mariconti [b], Rebecca Watts [a]

[a] Institute of Archaeology, University College London, 31-34 Gordon Sq, London, WC1H 0PY, United Kingdom
[b] Department of Security and Crime Science, University College London, 35 Tavistock Sq, London, WC1H 9EZ, United Kingdom

ARTICLE INFO

Keywords:
Curvature analysis
Auricular surface
Age estimation
Dirichlet normal energy
Intra-observer error

ABSTRACT

Traditional age estimation methods are prone to subjectivity, leading to a decrease in the reliability and repeatability of estimated ages in skeletal assemblages. In an attempt to reduce the level of subjectivity, this research applied a computational method designed to analyze surface topography, Dirichlet Normal Energy (DNE), to provide a mathematical assessment of age-related degeneration in the auricular surface. Reconstructed 3D models of 153 archaeological individuals were created by laser scanning and analyzed using the R studio package MolaR. DNE values showed moderate correlations with age phase (Buckberry-Chamberlain and Lovejoy), for the auricular surface as a whole as well as a number of topographical features (surface undulation, apical activity, macroporosity). Most encouragingly, this method had an extremely low levels of intra-observer error, which makes it repeatable and potentially more objective than traditional age estimation methods.

Introduction

In forensic investigations age estimation plays a crucial role in creating a biological profile to identify the decedent [1]. For adult individuals this is often based on progressive degenerative changes that occur at the sternal ends of the ribs [2], the pubic symphysis [3], and the auricular surface of the ilium [4,5]. However, there are concerns about the subjectivity of these traditional methods due to their qualitative nature which requires visual assessment of bones, a practice which relies on the observers' own experience to assess the level of degenerative change to a surface [6]. Studies which provide repeatability and reproducibility rates for these methods demonstrate that levels of intra- and inter-observer agreement rarely reach substantial (kappa=0.61-0.80) or almost perfect (0.81-1.00) levels of agreement [7–12], calling into question their value as age indicators when applied across multiple assemblages, or when the findings of different observers are compared. In order to reduce this subjectivity and improve levels of repeatability and reproducibility, researchers are making use of advances in computer imaging technology to develop objective methods of age estimation that can be analysed using quantitative, statistical models [13]. One such method that has shown promise is curvature analysis. This measures the degree to which a surface is curved or flat and is used to analyse subtle anomalies in the surface texture of an object or region of interest (ROI) [14,15]. Previous research has suggested that changes in the degree of curvature may be correlated with increasing age-at-death in the pubic symphysis and auricular surface [15–17]. The present research used a method of curvature analysis called Dirichlet Normal Energy (DNE) to assess the surface curvature in auricular surfaces which had been 3D reconstructed from laser scans of archaeological individuals. The aims were to; 1) identify and quantify the degree of expression for topographical features that are assessed during the application of traditional, macroscopic age estimation methods, and 2) test the repeatability of resultant DNE values to demonstrate their objectivity.

Age estimation using the auricular surface

While age-related changes to the auricular surface were first identified by Sashin [18], it was Lovejoy et al. [5] who proposed a method which categorized these changes according to age-at-death. This method consists of eight age phases which are delineated into five-year age categories based on the degree of expression of eight morphological features; granulation, density, microporosity, macroporosity, billowing, striation, apical activity, and activity in the retroauricular surface [5]. When tested on known-age skeletal samples this method has shown mixed results [12,19], with the main criticisms focusing on the lack of

* Corresponding author.
E-mail address: jisun.jang.19@ucl.ac.uk (J. Jang).

https://doi.org/10.1016/j.fri.2024.200579

Available online 19 January 2024

consistency between the eight features and the "optimistically narrow" ([4]:232) five-year categories. To address these limitations Buckberry and Chamberlain [4] developed a scoring system in which five morphological features, (transverse organization, surface texture, apical activity, macroporosity and microporosity), are assessed separately and each given a score of 1-3 or 1-5 based on their appearance and the proportion to which they extend over the auricular surface. The scores of each feature are then summed to produce a composite score which corresponds to one of seven stage phases, which each provide a mean age-at-death, standard deviation and age range. While the Buckberry-Chamberlain method performs better than the Lovejoy method on blind tests of known-age samples [20], a certain degree of subjectivity remains as the initial assessment relies on visual assessment of morphological features [9,10,21,22].

To further remove this subjectivity, it has been suggested that mathematical and computational approaches could be used to develop fully quantitative and user-independent methods [16,17,22]. For example, Slice and Algee-Hewitt [22] used a laser scanner to create three-dimensional models of pubic symphyses belonging to 41 known-age individuals from the W.M. Bass Skeletal Collection. Each model transformed the joint surface into a series of polygon faces, which allowed for the sampling of coordinates (x, y and z), at specific points. These were then analyzed through principal component analysis to identify eigenvalues that reflected measures of surface complexity. There was a statistically significant association between scores produced from the eigenvalues and known age-at-death, albeit with occasionally large differences between actual and estimated age [22]. However, tests for intra-observer variation were extremely encouraging, revealing that results from the repeated application of this methodology were "very consistent" ([22]: 842). Biwasaka et al. [16] also utilized 3D models of pubic symphyses, but to test the degree to which the curvature of the surface changed with age in a sample of 145 individuals from Japan. Mean curvature was calculated for every $5mm^2$ of the reconstructed surface and used to create a topographical map for each individual. Results showed an association between the degree of surface curvature and age-at-death, which was mainly attributed to the presence of horizontal ridges on the symphyseal surfaces of younger individuals producing high curvature values [16]. These ridges flattened out as age increased, a change that was reflected in lower curvature values for older individuals. However, fine surface features, such as pitting and porosity, could not be captured on the reconstructed models, limiting its ability to distinguish between older age groups. Stoyanova *et al.* [17] also examined associations between surface curvature and age-at-death in the pubic symphysis, but instead of producing topographical surface maps they used thin-plate splines to measure the amount of energy required to bend a theoretical flat plate to match the degree of curvature on the surface of a 3D model. After each model was standardized for size, orientation and position, the methodology was able to produce estimates of age-at-death which were broadly correlated with known-age, although the predictive ability reduced with increasing age [17]. However, repeatability rates were encouraging, with three rounds of repeated measures producing age estimates that never differed by more than three years for each of the 12 individuals in the sample [17]. Few published studies to date have applied a similar methodology to the auricular surface; Villa et al. [15] and Štepanovský et al. [23]. Villa et al. [15] used Gaussian curvature analysis to evaluate age-related changes in the degree of curvature for 98 auricular surfaces of known-age individuals from the Terry collection. Results showed a moderate correlation with age, with younger and older adults displaying high curvature values, while middle adults displayed lower values. Although the authors show that age-related morphological changes can be analysed on the reconstructed auricular surface, the specific criteria and the method to estimate the age were not provided [15]. Štepanovský et al. [23] created a novel age estimation software for use with 3D reconstructed auricular surfaces: CoxAGE3D. The process is fully automated within CoxAGE3D, improving levels of objectivity. To reduce statistical bias, the software was developed using a dataset of European and Asian individuals. However, information on repeatability and reproducibility was not provided in these publications [5,23].

Curvature analysis with dirichlet normal energy (DNE)

While computational methods of analysis are objective and appear to produce repeatable values, they are limited in their ability to capture finer topographical details in surface texture, making it difficult to identify certain features that are traditionally associated with later stages of age-related degeneration [15,16]. However, there are other methods of curvature analysis available which may negate this limitation. In 2011 DNE was first applied in the field of dental anthropology to aid in studies of dietary reconstruction by making topographic maps of tooth crown surfaces [14]. When applied to 3D models, DNE can identify subtle anomalies in the surface texture of an object by quantifying the deviation of the surface energy from a stable minimal energy state (i.e. it calculates how much the surface bends) [14]. To quantify the curvature, triangular polygons (3D structures composed of planes) are the focus of this analysis, rather than the true expression of curvature demonstrated by a surface. To perform DNE analysis, a 3D model of the surface should first be saved as a .ply file, which converts the normal surface into these polygons [14,24]. Each polygon face (ρ) consists of two principal curvatures representing the largest curvature and the smallest curvature ($\boldsymbol{\nu}$ and $\boldsymbol{\upsilon}$). The normal vector per vertex denotes the orthogonal vector from the vertex of the polygon (red arrow in Fig. 1). The normal vector is the average of the normal (blue line) of the adjacent polygons. When the normal vectors are translated to have common point, the polygon is formed having edge vectors ($\mathbf{n}_{\nu}$ and $\mathbf{n}_{\upsilon}$). The edge vectors are derivatives of the normal of v and u ([14]; Winchester, 2016) (Fig. 1).

Calculation of DNE starts by measuring the Dirichlet Energy Density (DED) at a polygon face (p) as demonstrated in the equation below ([24]:398):

$$DED(\rho) = (\mathbf{n}_{\nu})^2 + (\mathbf{n}_{\upsilon})^2$$
$$\mathrm{DNE} = \sum DED\left(\rho\right) x\ area\left(\rho\right)$$

If the surface becomes planar (flat), the surface energy moves to a stable minimal state. Consequently, the principal curvatures are closer to a value of 0. Conversely, if the surface has curvature or undulation, the DNE value increases [14,24]. DNE has several benefits over other methods of curvature analysis. Firstly, DNE is independent of the orientation of the object during the scanning phase (to create the 3D model) and does not always require landmarks to be placed on the models in order to perform measurements [14,24]. Both of these steps can be time-consuming and user-dependent, increasing the potential for intra- and inter-observer errors [25,26]. Furthermore, DNE calculates the degree of curvature more sensitively than other methods of curvature analysis [27]. Therefore by applying DNE, experiment time can be reduced, a user-independent method can be developed, and sensitive topographical surface features can be detected, making it a potentially useful tool in the analysis of age-related degenerative features to the auricular surface.

Materials

Auricular surfaces of adult individuals from the Chichester collection, a largely post-medieval archaeological assemblage stored at University College London, were used for the current research. As this is an archaeological collection no biographic information, (including age at death and sex) was available for the individuals. However, as the aims of this research were to identify and quantify the degree of expression of topographical features and to test the repeatability of DNE calculations, this was considered an appropriate dataset. Individual auricular surfaces were assigned to age phases based on the macroscopic criteria outlined by Lovejoy et al. [5] and Buckberry and Chamberlain [4]. Each specimen

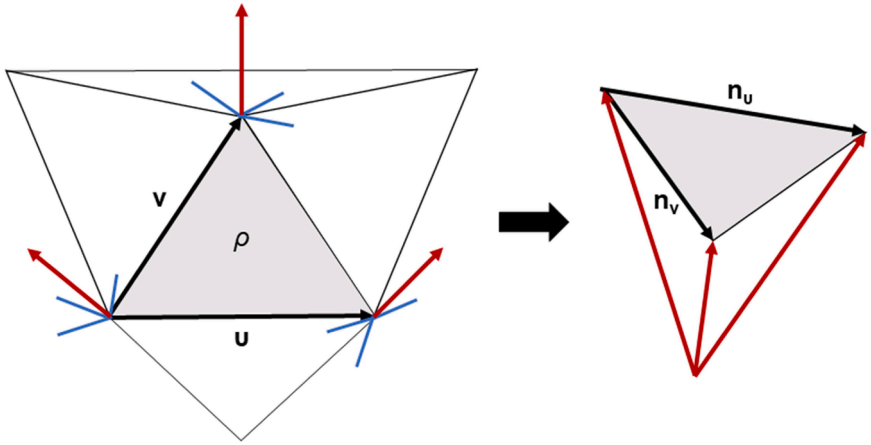

Fig. 1. Dirichlet Normal Energy.

was scored twice on two separate occasions by JJ. Only individuals that had been scored as the same age phase in both assessments (n=153; female=69, male=84) were used for DNE analysis. Reconstructed 3D models were analyzed by these age phase groups in order to test for relationships between DNE values and the age-related degenerative features used by traditional age estimation methods.

Method

Scanning and modeling

An EinScan-SP laser scanner (camera resolution 1.3 megapixels) was used to take scans of each auricular surface. Pelves were placed on the turntable with the auricular surface facing the scanner, and each specimen was scanned from a minimum of five angles to construct a clear image of the whole surface (including features in depressed areas). The separate images were aligned and merged automatically by the software EXScanS_v3.1.0.1 to produce a single 3D model which was saved as a .ply file. Each model was then edited manually to isolate the auricular surface and remove any non-articular regions of bone (using the outer margin of the auricular surface as a guide). The final auricular surface .ply files were not subjected to any trimming processes such as simplification, smoothing or sharpening.

Calculation of DNE values

Each .ply file was opened in R studio and the boundary of the auricular surface was determined using the BoundaryDiscard code to delineate the ROI. DNE was then calculated using the MolaR package [24]. This provided output files containing information for DED, area, and face indexes from the original .ply file. The output files were exported as a CSV file using the 'write.xlsx' function. In the saved CSV file, detailed DNE was calculated by multiplying DED and area for each ROI. As auricular surface sizes varied throughout the dataset, the number of polygon faces in each .ply file also varied (i.e. larger auricular surfaces had a greater number of polygon faces). To perform comparisons, this condition had to be the same and therefore the total DNE of each surface was divided by the number of polygon faces to provide standardization.

Finding Face indexes

To calculate DNE for each topographical feature, the ROI had to be determined manually. This was not possible in R studio so each .ply file was opened in MeshLab and the selecting tool was used to manually select the relevant ROI, based on visual identification. Each topographical feature was identified according to the descriptions provided by Lovejoy et al. [5] and Buckberry and Chamberlain [4]. To be precise, surface undulation involved selecting areas of the auricular surface where striae and billows were visible. Thus, most transverse undulations on the surface were selected regardless of the degree. Areas displaying visible pores over 1mm in diameter were selected as macroporosity. Apical regions consisted of polygons located within 1cm to the left and right sides of the termination of the arcuate line. Once the ROI was selected the exact number of face indexes could be identified and cross-referenced with the CSV file to calculate their DNE values (Fig. 2).

Analysis

Statistical analyses were carried out in Excel. Spearman's correlation was used to test for correlations between age phase and DNE values for the auricular surface as a whole (total DNE/total polygon face), and for the topographical features surface undulation, apical activity, and macroporosity (polygon face belonging to macroporosity DNE/total polygon face). Prior to these analyses independent t-tests were performed to test for differences in DNE values between males and females (p=0.32), and between the left and right auricular surfaces of each individual (p=0.17). As there were no significant differences these datasets could be combined for analysis. QQ plots and Levene's test for equality of variances were applied first to ensure that these datasets were normally distributed and had equal variances (which was the case). All 153 individuals were re-scanned and re-analyzed (by JJ) according to the same methodological procedure one month after the original analyses took place in order to test the intra-observer error. DNE values from the first and second analyses were compared using the concordance correlation coefficient ($p(c)$) in Excel.

Results

DNE values could be calculated for each auricular surface as a whole. It was also possible to identify and calculate DNE values for the following topographical features; surface undulation, apical activity and macroporosity. The figures below show the median and range of variation in DNE values for the total auricular surface and the individual topographical features, arranged by the Lovejoy et al. [5] and Buckberry and Chamberlain [4] age phases.

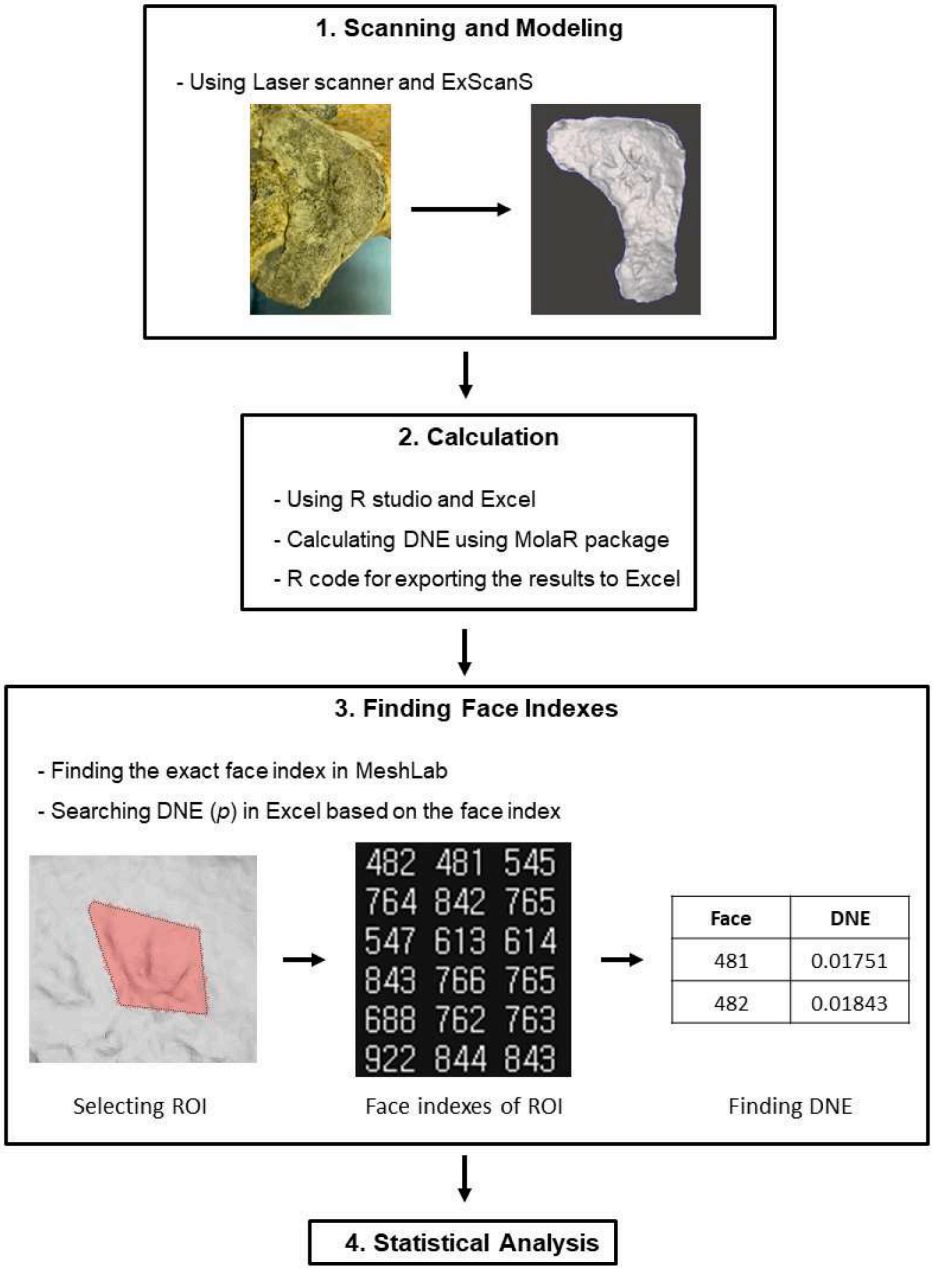

Fig. 2. Workflow for DNE method.

Total DNE/total polygon face

Across the whole dataset DNE values of the auricular surface ranged from 0.009 to 0.039. When split by age phase the Lovejoy and Buckberry-Chamberlain methods showed similar parabola tendencies (Figs. 3 and 4) with age phase 1 producing median DNE values of 0.0189 and 0.0182 (respectively), while age phases 2-5 produced median DNE values between 0.0134 and 0.0156. Median DNE values then increased in the later age phases (phases 6-8 in the Lovejoy method, and phases 6-7 in the Buckberry-Chamberlain method). The highest DNE values were observed in the final phase for both methods. Although there was a considerable degree of overlap between many of the age phases, according to Spearman's correlation there were moderate correlations between DNE value and age phase for both the Lovejoy method ($p<0.05$, $r_s=0.52$) and the Buckberry-Chamberlain method ($p<0.05$, $r_s=0.54$).

Surface undulation

There was a moderate correlation between DNE values for surface undulation and age phase for the Lovejoy method (Spearman's correlation $p<0.05$, $r_s=-0.41$), as despite a small increase in phase 7, median DNE values consistently decreased from 0.1824 in phase 1 to 0.0630 in phase 8 (Fig. 5). While indicating that surface undulation was relatively minor (i.e. flat) in all age phases, this does reflect age-related loss of billowing and transverse organization, suggesting that the surface becomes even flatter as age phase increases. DNE values for surface undulation scored using the Buckberry-Chamberlain method demonstrated a similar tendency (Fig. 6). However, according to Spearman's correlation, this did not reach statistical significance ($p=0.20$, >0.05). The component score Fig. 7 did not produce a significant correlation either ($p=0.32$, >0.05).

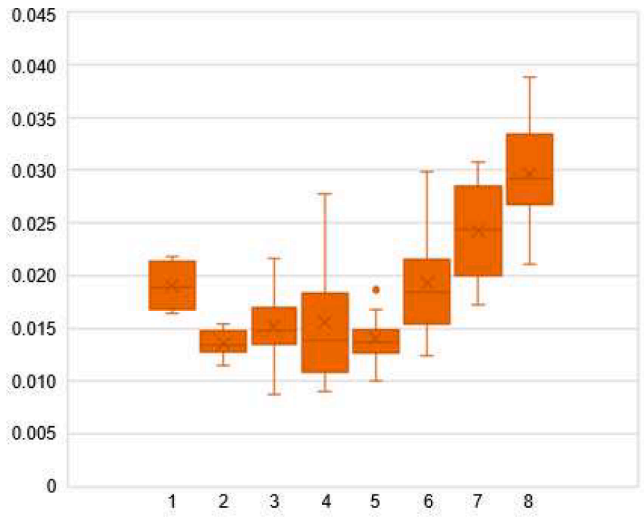

Fig. 3. Total DNE/total polygon faces for each age phase of the Lovejoy method.

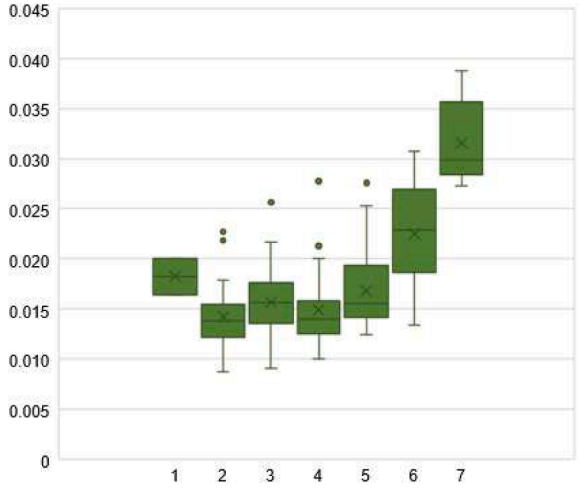

Fig. 4. Total DNE/polygon faces for each age phase of the Buckberry-Chamberlain method.

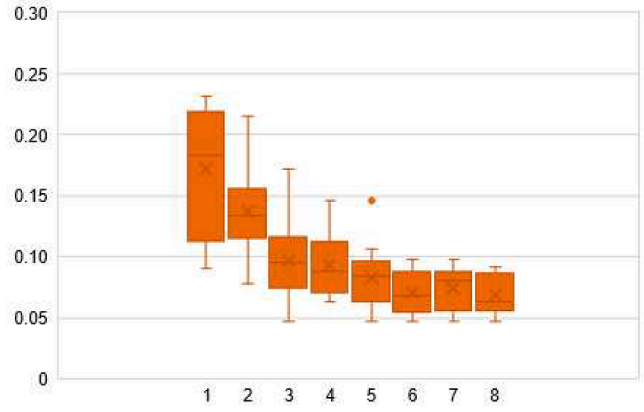

Fig. 5. Surface undulation for each age phase of the Lovejoy method.

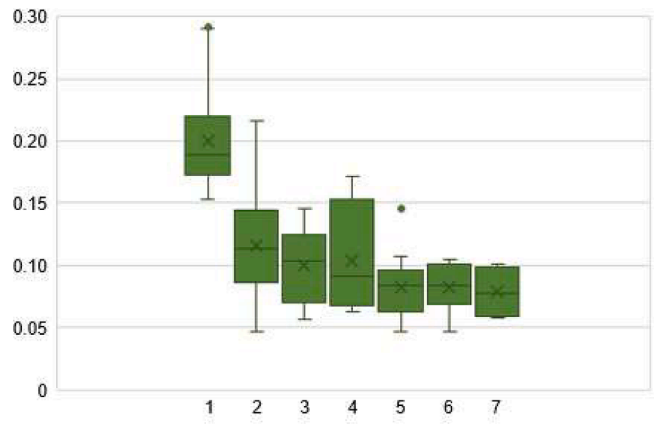

Fig. 6. Surface undulation for each age phase of the Buckberry-Chamberlain method.

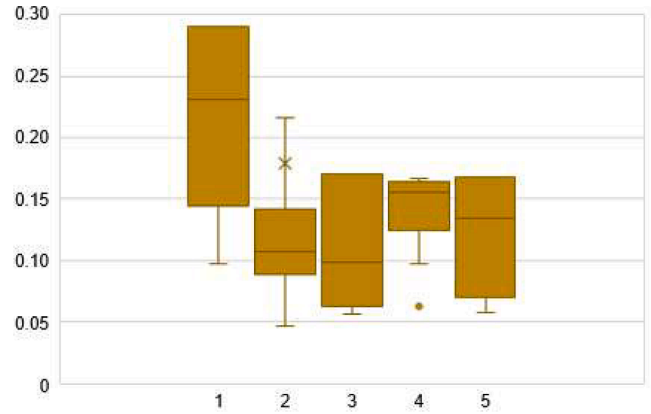

Fig. 7. Surface undulation for each component score of the Buckberry-Chamberlain method.

Apical activity

For both methods, median DNE values were consistently low (0.2342-0.3615) for age phases 1-5 (Figs. 8 and 9) and increased in later phases; 0.4442-0.5918 for phases 6-8 of the Lovejoy method, and 0.4521-0.5918 for phases 6-7 of the Buckberry-Chamberlain method. This represents the increasing degree of curvature as the margins of the apex become more lipped and irregular with increasing age phase. When categorizing DNE by the component score from the Buckberry-

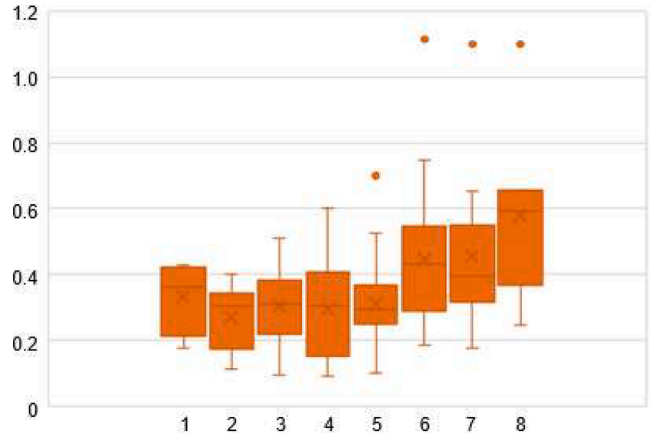

Fig. 8. Apical activity for each age phase of the Lovejoy method.

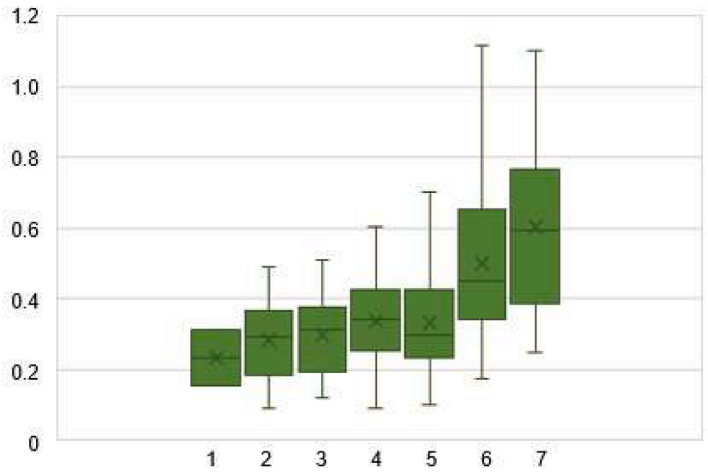

Fig. 9. Apical activity for each age phase of the Buckberry-Chamberlain method.

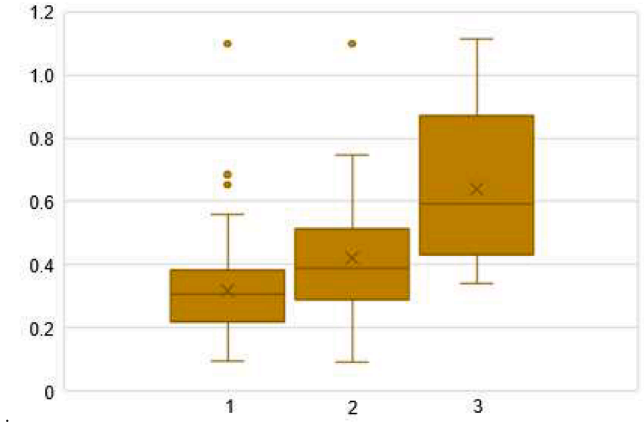

Fig. 10. Apical activity for each component score of the Buckberry-Chamberlain method.

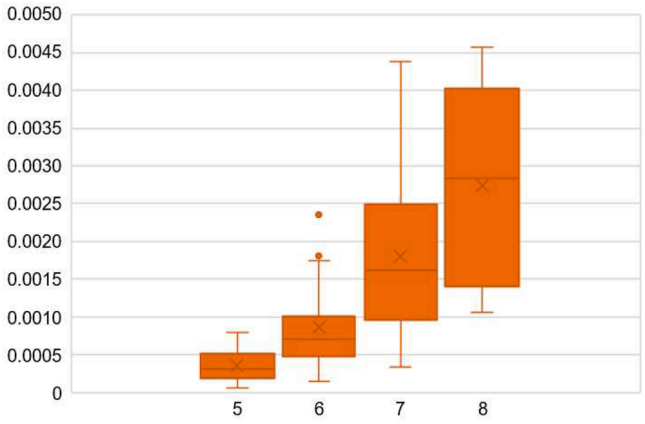

Fig. 11. Macroporosity for each age phase (5 to 8) of the Lovejoy method.

Chamberlain method, a positive linear tendency was shown (Fig. 10). According to Spearman's correlation there were moderate correlations between apical activity and age phase for the Lovejoy method ($p<0.05$, $r_s=0.37$) and the Buckberry-Chamberlain method ($p<0.05$, $r_s=0.40$), and a weak correlation with the component score ($p<0.05$, $r_s=0.46$).

Macroporosity

In age phases 1-4, macroporosity was not visible on the bone surfaces of the auricular surfaces, or the resultant 3D models, in either of the methods. Consequently, this topographic feature could only be analyzed in age phases 5-8. Positive linear tendencies were observed for both methods and the Buckberry-Chamberlain component scores (Figs. 11, 12, and 13). Median values increased from 0.00031 in age phase 5 to 0.00284 in age phase 8 (Lovejoy method) and 0.00325 in age phase 7 (Buckberry-Chamberlain method). This represents the higher degree of curvature caused by large pores interrupting the integrity of the auricular surface. Spearman's correlation demonstrated that macroporosity and age phase were strongly correlated for the Lovejoy method ($p<0.05$, $r_s=0.73$). The Buckberry-Chamberlain method ($p<0.05$, $r_s=0.61$), and the component score ($p<0.05$, $r_s=0.50$) had moderate correlations.

Intra-observer error

The concordance correlation coefficients ($p(c)$) of total DNE/total polygon face, surface undulation, apical activity, and macroporosity

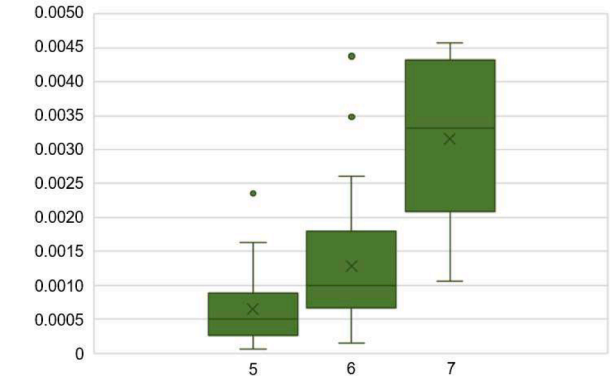

Fig. 12. Macroporosity for each age phase (5 to 7) of the Buckberry-Chamberlain method.

were 0.91, 0.89, 0.85, and 0.97 respectively (Table 1), demonstrating fairly good to excellent levels of agreement.

Discussion and Conclusion

The following topographic features, assessed as age-related degenerative features in the Lovejoy et al. [5] and Buckberry and Chamberlain [4] methods, could be identified and quantified via DNE analysis using 3D reconstructed laser scans of auricular surfaces; surface undulation,

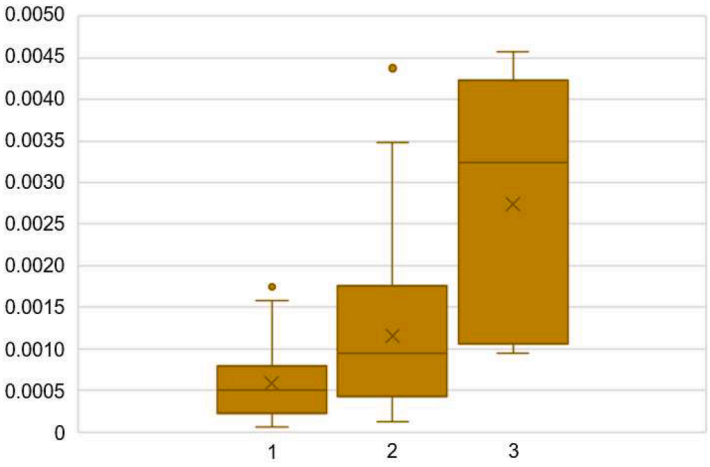

Fig. 13. Macroporosity for each component score of the Buckberry-Chamberlain method.

Table 1
The concordance correlation coefficient (*p(c)*) to verify the intra-observer error.

	μ_x	σ_x	μ_y	σ_y	p	$p(c)$	**Interpretation**
Total DNE /Total polygon face	0.0176	0.0055	0.0171	0.0057	0.9195	0.9166	Very good
Surface undulation	0.1437	0.0650	0.1374	0.0650	0.8978	0.8936	Fairly good
Apical activity	0.3806	0.1911	0.3370	0.1886	0.8744	0.8505	Fairly good
Macroporosity	11.4396	10.5311	9.9043	9.7800	0.9896	0.9758	Excellent

apical activity and macroporosity. It was not possible to detect microporosity (another age-related feature) as the level of detail in the 3D reconstructions was not great enough to reproduce this fine change in surface texture. Similarly, the feature 'granulation' could not be assessed as this is a purely visual feature which does not affect surface curvature [15]. In addition to the three topographical features, it was also possible to calculate DNE values for the auricular surface as a whole. Considering all t-test results, the auricular surface had no significant sex or side differences in DNE. This is in accordance with results reported in previous studies [4,5,19]. Intra-observer error tests revealed that DNE values were highly repeatable, with values for the total surface and all three topographical features showing almost perfect levels of agreement between the first and second analyses. This suggests that subtle anomalies in the topography of the auricular surface can be captured and quantified by DNE, producing highly repeatable results when analyzed by the same observer.

When DNE values were analyzed according to the Lovejoy et al. [5] and Buckberry and Chamberlain [4] age phases, a number of significant correlations were observed. In terms of surface undulation, the earliest phases (1-5) of the Lovejoy method produced higher DNE values than the later phases (6-8). This is most likely due to the distinct transverse organization that characterizes the more youthful auricular surface creating departures from a stable minimal state in the surface energy. As the degree of transverse organization decreases with increasing age [5], the auricular surface becomes relatively flatter, creating a more stable energy state, and the resultant DNE values also decrease. Age phases from the Buckberry-Chamberlain [4] method also showed this general trend of decreasing DNE values, but the association did not reach statistical significance.

Apical activity is absent or minimal in Lovejoy phases 1–4, and rarely appears in younger individuals according to the Buckberry-Chamberlain method [4,5]. Changes develop and become more marked (i.e. the apex becomes more lipped and irregular) in the later age phases. This was reflected in the relatively low apical DNE values for age phases 1–5, reflecting surface textures that were closer to a stable minimal energy state. DNE values then increased for age phases 6–8, capturing the increasing degree of curvature as the apex becomes more irregular [5]. Macroporosity demonstrated a similar tendency; this feature did not appear until age phase 5 for either method, but when it was present, produced values above 0.0004. Median values then increased with increasing age phase, reflecting the increasing curvature of the surface.

The total DNE value/total polygon face number includes information about the three topographical features as it analyses the curvature of the auricular surface as a whole. Surface undulation appears to have the greatest impact on surface energy state for the earlier age phases as even though these auricular surfaces are relatively flat, the billowing and transverse organization create small departures from a stable energy state. The loss of billowing in age phases 2–5 means that the surface becomes even flatter, and is reflected by the observable decrease in DNE values. The development of apical activity and macroporosity after age phase 5 contributes to the breakdown of the surface and the texture becomes more curved, reflected again in the increasing DNE values for age phases 6–8.

These results show that subtle changes in the texture of the auricular surface, including features which have been traditionally associated with age-at-death estimation, can be identified and quantified with DNE. Surface undulation, apical activity, macroporosity, and the total DNE/total polygon face all produced DNE values which were broadly correlated with age phases from the Lovejoy and Buckberry-Chamberlain methods. Moreover, these values are extremely repeatable, with DNE values produced on two separate occasions showing almost perfect levels of agreement for each of the features examined. However, large overlaps in the range of DNE values shown by each age phase mean that it is currently not possible to estimate age by this measure alone. This was demonstrated particularly clearly in the middle age phases (2–5), where the limits of the equipment's performance meant that changes in microporosity and surface granulation, traditional criteria for distinguishing between these phases, could not be identified.

Furthermore, although the current study produced low levels of intra–observer error, the method still has the potential for subjectivity, particularly in the calculation of DNE values for topographical features which require the ROI to be delineated manually by the user in Meshlab.

It may be possible to overcome this drawback by removing the need to focus on visual features altogether and focusing on mathematical features of the auricular surface instead. For example, MolaR can calculate the percentage of the surface that is mathematically flat (DNE=0), or demonstrates higher levels of curvature (DNE >= 0.6). A more fruitful avenue for future research may be to examine how these features correlate with age-at-death in known-age skeletons as a further step towards a completely objective and user-independent method of age estimation (Fig. 7).

CRediT authorship contribution statement

Jisun Jang: Conceptualization, Data curation, Formal analysis, Investigation, Methodology, Project administration, Validation, Writing – original draft, Writing – review & editing. **Enrico Mariconti:** Methodology, Writing – original draft. **Rebecca Watts:** Project administration, Writing – original draft, Writing – review & editing.

Declaration of competing interest

The authors declare that they have no known competing financial interests or personal relationships that could have appeared to influence the work reported in this paper.

Acknowledgements

We would like to thanks the reviewers for their constructive comments which greatly improved this manuscript.

References

[1] L.L. Klepinger, Fundamentals of Forensic Anthropology, Wiley-Liss, Hoboken, 2006.
[2] M.Y. Iscan, S.R. Loth, M.Y. Iscan, Osteological manifestations of age in the adult, in: L.A.R. Kennedy (Ed.), Skeletal biology of past peoples: research methods, Wiley-Liss, New York, 1989, pp. 189–224.
[3] S. Brooks, J.M. Suchey, Skeletal age determination based on the os pubis: A comparison of the Acsadi-Nemeskeri and Suchey-Brooks methods, Hum. Evol. 5/3 (1990) 227–238.
[4] J.L. Buckberry, A.T. Chamberlain, Age estimation from the auricular surface of the ilium: A revised method, Am. J. Phys. Anthropol. 119/3 (2002) 231–239, https://doi.org/10.1002/ajpa.10130.
[5] C.O. Lovejoy, R.S. Meindl, T.R. Pryzbeck, R.P. Mensforth, Chronological metamorphosis of the auricular surface of the ilium: A new method for the determination of adult skeletal age at death, Am. J. Phys. Anthropol. (68/1) (1985) 15–28, https://doi.org/10.1002/ajpa.1330680103.
[6] H.M. Garvin, N.V. Passalacqua, Current practices by forensic anthropologists in adult skeletal age estimation, J. Forensic Sci. 57/2 (2012) 427–433, https://doi.org/10.1111/j.1556-4029.2011.01979.x.
[7] P. Intasuwan, P. Palee, A. Sinthubua, P. Mahakkanukrauh, Efficiency of dry bone inspection compared with two-dimensional os coxal images for age estimation in a Thai population, Veterinary Integrative Sci. 20 (2022) 185–197.
[8] M. Jones, G.G.D. Brits, Age estimation accuracies from black South African os coxae, J. Comparative Human Biol. 69 (2018) 248–258.
[9] E. Michopoulou, P. Negre, E. Nikita, E.F. Kranioti, The auricular surface as age indicator in a modern Greek sample: A test of two qualitative methods, Forensic Sci. Int. 280 (2017), https://doi.org/10.1016/j.forsciint.2017.08.004, 246.e1-246.e7.
[10] K. Moraitis, E. Zorba, C. Eliopoulos, S.C. Fox, A test of the revised auricular surface aging method on a modern European population, J. Forensic Sci. (59/1) (2014) 188–194, https://doi.org/10.1111/1556-4029.12303.
[11] J. Rivera-Sandoval, T. Monsalve, C Cattaneo, A test of four innominate bone age assessment methods in a modern skeletal collection from Medellin, Colombia, Forensic Sci. Int. 282 (2018), 232.e1-232.e8.
[12] S.R. Saunders, C. Fitzgerald, T. Rogers, C. Dudar, H. McKillop, A test of several methods of skeletal age estimation using a documented archaeological sample, Canadian Soci. Forensic Sci. J. (25/2) (1992) 97–118, https://doi.org/10.1080/00085030.1992.10757005.
[13] A. Schmitt, Une nouvelle méthode pour estimer l'âge au décès des adultes à partir de la surface sacro-pelvienne iliaque, Bulletins et Memoires de la Societe d' Anthropologie de Paris 17 (2005) 29–101, https://doi.org/10.4000/bmsap.943.
[14] J.M. Bunn, D.M. Boyer, Y. Lipman, E.M. St.Clair, J. Jernvall, I. Daubechies, Comparing dirichlet normal surface energy of tooth crowns, a new technique of molar shape quantification for dietary inference, with previous methods in isolation and in combination, Am. J. Phys. Anthropol. 145/2 (2011) 247–261, https://doi.org/10.1002/ajpa.21489.
[15] C. Villa, J. Buckberry, C. Cattaneo, B. Frohlich, N. Lynnerup, Quantitative analysis of the morphological changes of the pubic symphyseal face and the auricular surface and implications for age at death estimation, J. Forensic Sci. 60/3 (2015) 556–565, https://doi.org/10.1111/1556-4029.12689.
[16] H. Biwasaka, K. Sato, Y. Aoki, H. Kato, Y. Maeno, T. Tanijiri, S. Fujita, K. Dewa, Three dimensional surface analyses of pubic symphyseal faces of contemporary Japanese reconstructed with 3D digitized scanner, Leg. Med. (2013) 264–268, https://doi.org/10.1016/j.legalmed.2013.02.003, 15/5.
[17] D. Stoyanova, B.F.B. Algee-Hewitt, D.E. Slice, An enhanced computational method for age-at-death estimation based on the pubic symphysis using 3D laser scans and thin plate splines, Am. J. Phys. Anthropol. 158/3 (2015) 431–440, https://doi.org/10.1002/ajpa.22797.
[18] D.A. Sashin, Critical analysis of the anatomy and the pathological changes of the sacroiliac joint, J. Bone Joint Surg. 12 (1930) 891–910.
[19] D.L. Osborne, T.L. Simmons, S.P. Nawrocki, Reconsidering the auricular surface as an indicator of age at death, J. Forensic Sci. (49/5) (2004) 905–911.
[20] C. Falys, H. Schutkowski, D.A. Weston, Auricular surface aging: worse than expected? A test of the revised method on a documented historic skeletal assemblage, Am. J. Phys. Anthropol. 130 (2006) 508–513.
[21] R.R. Paine, J.L. Boldsen, Linking Age-at-Death distributions and ancient population dynamics: a case study, in: R.D. Hoppa (Ed.), Paleodemography Age Distributions from Skeletal Samples, Cambridge University Press, Cambridge, 2002, pp. 169–180.
[22] D.E. Slice, B.F.B. Algee-Hewitt, Modeling bone surface morphology: a fully quantitative method for age-at-death estimation using the pubic symphysis, J. Forensic Sci. 60/4 (2015) 835–843, https://doi.org/10.1111/1556-4029.12778.
[23] M. Štepanovský, Z. Buk, A.P. Kotěrová, J. Brůžek, Š. Bejdová, N. Techataweewan, J. Velemínská, Automated age-at-death estimation from 3D surface scans of the facies auricularis of the pelvic bone, Forensic Sci. Int. (2023) 349, https://doi.org/10.1016/j.forsciint.2023.111765.
[24] J.D. Pampush, J.M. Winchester, P.E. Morse, A.Q. Vining, D.M. Boyer, R.F. Kay, Introducing molaR: a new r package for quantitative topographic analysis of teeth (and other topographic surfaces), J. Mamm. Evol. (23/4) (2016) 397–412, https://doi.org/10.1007/s10914-016-9326-0.
[25] P. Gunz, P. Mitteroecker, F.L. Bookstein, Semilandmarks in three dimensions, in: D. E. Slice (Ed.), Modern Morphometrics in Physical Anthropology. Developments in Primatology: Progress and Prospects, Springer, Boston, MA, 2005, pp. 73–98.
[26] P.D. Polly, N. McLeod, Locomotion in fossil carnivora: an application of eigensurface analysis for morphometric comparison of 3D surface, Palaeontologia Electronica (11/2) (2008) 1–13. Available at: http://palaeo-electronica.org/2008_2/135/index.html.
[27] L.R. Godfrey, J.M. Winchester, S.J. King, D.M. Boyer, J. Jernvall, Dental topography indicates ecological contraction of lemur communities, Am. J. Phys. Anthropol. 148/2 (2012) 215–227, https://doi.org/10.1002/ajpa.21615.